Journal of Physics: Conference Series **632** (2015) 012033 doi:10.1088/1742-6596/632/1/012033

Searches for point-like sources using 2007-2012 data from the ANTARES neutrino telescope

Javier Barrios-Martí, on behalf of the ANTARES Collaboration

Instituto de Física Corpuscular (CSIC - UV), C/Catedrático José Beltrán, 2, E-46980 Paterna, Spain

E-mail: javier.barrios@ific.uv.es

Abstract. A search for point-like sources of cosmic neutrinos has been performed using the 2007 to 2012 data collected by the ANTARES neutrino telescope. The search is performed by looking for accumulations of muon neutrinos over the expected atmospheric background. No clear signal has been found. The cluster of events with the highest significance (2.2σ) was found at equatorial coordinates (RA, DEC) = ($-46.8°$, $-64.9°$). Furthermore, 90% confidence level upper-limits have been set for 50 pre-selected astrophysical neutrino source candidates for an E^{-2} flux normalization. In addition, due to the accumulation of 7 high energy neutrinos close to the Galactic Centre recently reported by the IceCube collaboration, a specific search around 20° from the Galactic Centre has been performed. No evidence of a signal has been found in the ANTARES data within this region.

1. Introduction

The aim of neutrino telescopes is to observe the universe with the use of neutrinos, which have advantageous properties compared to other stable particles. Cosmic rays may be deflected by magnetic fields and therefore lose the information about their origin, while the mean free path of high energy photons heavily depends on their energy. Neutrinos are neutral and weakly interacting particles, so they point directly back to their origin. A first signal of cosmic neutrinos has been reported by IceCube [1, 2], which includes a cluster of events close to the Galactic Centre. Even if this cluster is not statistically significant, some authors have suggested they may be due to a single point source [3]. Due to its location in the Mediterranean Sea, the better muon rejection efficiency of the Southern Hemisphere provides a better sensitivity to Galactic sources with energies < 100 TeV. This fact is especially important for the interpretation of the observed cluster of events close to the Galactic Centre by IceCube.

2. The ANTARES neutrino telescope

The ANTARES neutrino telescope is the first neutrino telescope which operates in the Mediterranean Sea. It is located 40 km to the South of Toulon (France), at the coordinates (42° 48' N, 6° 10' E) [4]. It consists of 12 lines of 350 m with a buoy on the top to keep them vertical. Each line contains 25 storeys with 3 Optical Modules (OMs). An Optical Module constists of a photomultiplier tube (PMT) of 10" inside a glass sphere of 17". These OMs are facing downwards at an angle of 45° in order to optimize the detection of upgoing muon-neutrinos.

The detection principle is based on the indirect detection of high energy neutrinos which interact via charged current (CC) interaction with a nucleus (N) inside or nearby the detector volume:

$$\nu_l + N \rightarrow l^- + X; \;\; \bar{\nu}_l + N \rightarrow l^+ + X, \tag{1}$$

where a charged lepton and an hadronic shower are produced. In case this lepton is a muon, it can travel a long distance before decaying. Since this muon is travelling at relativistic speeds, it will emit Cherenkov radiation. Some of the emitted photons are detected by the PMTs, producing a signal ("hit") with the corresponding charge and time information. The information collected by the hits of a muon is used to reconstruct the direction of the muon.

3. Data selection

The data considered for this analysis was collected between January 29, 2007 to December 31, 2012. The total measurement period comprises a livetime of 1338 days, which is 70% larger compared to the previous ANTARES point-source analysis [5].

Using the hit and time position information of hits, triggered events are reconstructed. This reconstruction is done by means of a maximum likelihood (ML) method [6]. The procedure is based on a multi-step procedure to fit the direction of the reconstructed muon by maximising the ML-parameter Λ, which indicates the goodness of the reconstruction. Furthermore, the estimated uncertainty of the track direction, β, is computed from the covariance matrix.

The KM3 package [7] is used to simulate the muon propagation. Additionaly, the simulation of neutrinos and atmospheric muons is performed with the GENHEN [7] and MUPAGE [8, 9] packages, respectively. The Bartol flux [10] is used for the atmospheric neutrino simulation. In order to test our simulations, a comparison of the Λ distribution in the data and simulated samples is performed. Figure 1 shows to the comparison for zenith angles θ with $\cos\theta < 0.1$, where $0^\circ < \theta < 90^\circ$ correspond to down-going tracks, and $90^\circ < \theta < 180^\circ$ to up-going tracks.

Before performing the analysis on data, events are selected by following a blind procedure on pseudo-experiments. The final sample is chosen so that it minimises the neutrino flux needed for a 5σ discovery in 50% of the experiments for a E^{-2} source spectrum. The final cuts correspond to $\Lambda > -5.2$, $\beta < 1^\circ$ and $\cos\theta < 0.1$, which leads to a total number of 5516 events. The estimated contamination of mis-reconstructed amospheric muons is 10%.

4. Performance of the detector

The cumulative distribution of the angular resolution can be calculated to show the pointing accuracy of the detector. The angular resolution of each event, Ψ, is defined as the difference between the true simulated direction and its reconstructed track. Figure 2 shows both the distribution for the current (blue) and previous (dashed red line) analysis [5]. Due to an improvement on the modelling of the PMT transit-time distribution the calculation of the median angular resolution is 0.38°, which corresponds to a 15% improvement.

The "acceptance" of the detector is calculated in order to obtain the number of signal events for a given source assumption. Multiplied by a given flux normalisation, Φ_0, it returns the number of cosmic neutrinos from a source. It depends on the detector effective area for a given selection cut, A_{eff}; the source energy spectrum and declination. The acceptance for a given declination, δ, can be described as

$$A(\delta) = \Phi_0^{-1} \int dt \int dE_\nu A_{eff}(E_\nu, \delta) \frac{d\Phi}{dE_\nu} \, . \tag{2}$$

For this analysis, the time integration covers the whole livetime of 1338 days, and the assumed energy spectrum is $\frac{d\Phi}{dE_\nu} = \Phi_0 E_\nu^{-2}$. The acceptance as a function of the declination δ is calculated and shown in Figure 3.

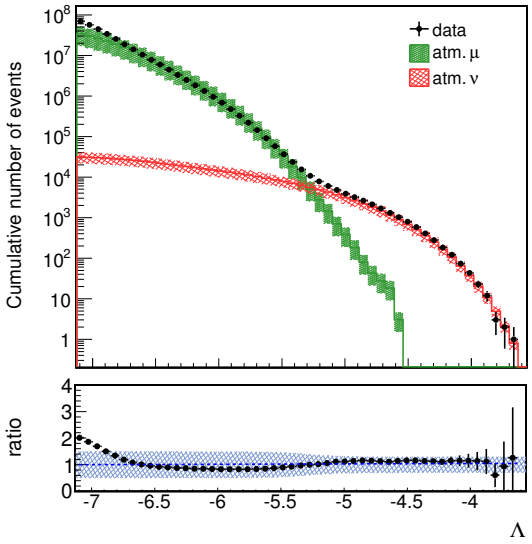

Figure 1. Cumulative distribution of the track reconstruction quality parameter, Λ, for tracks with an angular error estimate $\beta < 1^\circ$ and coming from a direction $\cos\theta < 0.1$ (mostly upgoing). A better track reconstruction is given by larger values of Λ. Since no upgoing atmospheric muons are expected, muon-neutrinos are expected to dominate the region with larger Λ values. The ratio between data and simulation is given in the bottom panel. Data is indicated by black dots, whose uncertainties are calculated from statistical errors. The red (green) distribution indicates the simulated atmospheric neutrinos (muons), where a 30% (50%) relative error was assigned [11, 12].

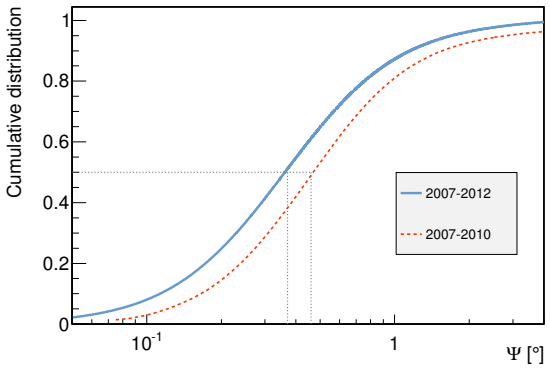

Figure 2. Neutrino angular resolution determined as the median of the cumulative distribution of the reconstruction angle, Ψ, for the present data (solid blue line) compared to the 2007-2010 analysis (dashed red line). The black-dotted line indicates the median value.

5. Search for cosmic neutrino sources

Atmospheric neutrino events are distributed isotropically, whereas cosmic neutrinos are expected to accumulate in clusters. A maximum-likelihood estimation is done in order to search for signal events. This likelihood describes the data in terms of background and signal probability density functions (PDFs):

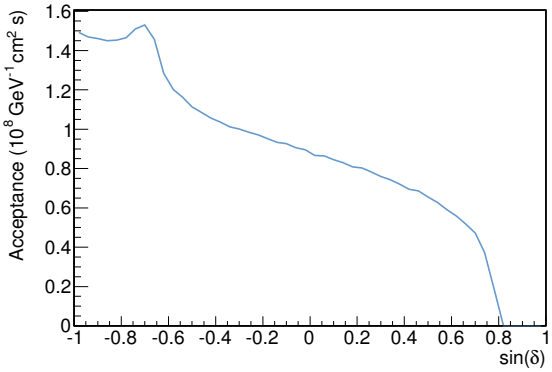

Figure 3. Acceptance (defined in Equation 2) for events passing the final selection cuts. An E^{-2} source spectrum has been assumed for the calculation.

$$\log L_{s+b} = \sum_i \log \left[\frac{n_s}{N} S_i + \left(1 - \frac{n_s}{N}\right) B_i \right], \tag{3}$$

where B_i and S_i denote the background and signal PDFs for the ith event, respectively, N indicates the events in the sample, and n_s represents the fitted number of signal source events. The signal PDF is defined as

$$S_i = \frac{1}{2\pi\beta_i^2} \exp\left(-\frac{\psi_i(\vec{x}_s)^2}{2\beta_i^2}\right) P_s(\mathcal{N}_i^{hits}, \beta_i), \tag{4}$$

where $\psi_i(\vec{x}_s)^2$ denotes the angular distance of an event i to the source direction, $\vec{x}_s = (\alpha_s, \delta_s)$, and $P_s(\mathcal{N}_i^{hits}, \beta_i)$ gives the probability for a signal event to be reconstructed with a number of hits $\mathcal{N}_i^{hits}$ and an angular error estimate of β_i.

The background PDF is defined as

$$B_i = \frac{B(\delta_i)}{2\pi} P_b(\mathcal{N}_i^{hits}, \beta_i), \tag{5}$$

where $P_b(\mathcal{N}_i^{hits}, \beta_i)$ indicates the probability for a background event to be reconstructed with an angular error estimate of β_i and a number of hits $\mathcal{N}_i^{hits}$, and $B(\delta_i)$ is the probability for an event to be at a declination δ_i.

In order to determine the significance of any cluster, the test statistic, TS, is defined as TS = $\log L_{s+b} - \log L_b$. L_b indicates the value of the likelihood for the case of no signal events ($n_s = 0$). Larger values of the TS designate a smaller probability of the cluster to be generated from only atmospheric events.

6. Results of the full-sky and candidate list searches

The full-sky search consists of an exploration for a significant cluster of signal events anywhere in the ANTARES visible sky. First, all clusters with at least 4 events in a half-opening angle cone of 3° are pre-selected. The likelihood, L_{s+b}, is maximised for each of them by adjusting the free parameters $\vec{x}s$ and n_s. The most significant accumulation of events of the full-sky search is located at $(\alpha, \delta) = (-46.8°, -64.9°)$. This location is compatible with the direction of the most significant accumulation found in the 2007-2010 analysis. This cluster has a post-trial p-value of 2.7% (significance of 2.2σ in the two-sided convention). The number of fitted events is $n_s = 6.2$.

6 (14) events are found in a cone of 1° (3°) from the fitted centre of the cluster. No significant excess was found. The upper limits at the 90% confidence level (C.L.) from point-sources are presented by the light blue-dashed line in Figure 5, where each dot indicates the highest upper-limit in declination bands of 1°. Figure 4 shows the p-values of the whole visible sky in steps of 0.2° in right ascension and declination.

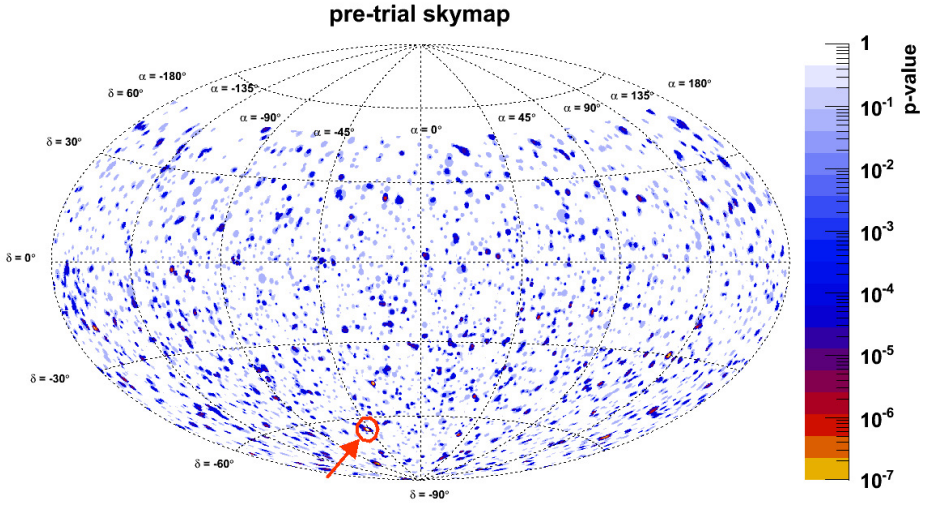

Figure 4. Pre-trial p-values of the ANTARES visible sky.

In the candidate list search, the TS is evaluated at the position of 50 neutrino candidate sources. The most significant accumulation of this search was found at the position of HESS J0632+057. The post-trial p-value is 6.1% (significance of 1.9σ) for a fitted number of source events of $n_s = 1.6$. The complete list of these sources with their corresponding flux upper limits and pre-trial p-values is shown in Table 1. Furthermore, the upper-limits and the overall fixed-source sensitivity are also represented in Figure 5, where the upper limits and sensitivities are calculated by using the Neyman method [14] at a 90% C.L.

7. Search for cosmic sources around the Galactic Centre

After the recent evidence of an excess of high energy neutrinos by IceCube [1], the presence of a point source at equatorial coordinates $\alpha = -79°$, $\delta = -23°$ has been proposed [3] in order to justify the accumulation of seven events close to the Galactic Centre. A flux normalisation of $\Phi_0 = 6 \times 10^{-8}$ GeVcm^{-2}s^{-1} would therefore be expected for this hypothetical source.

Due to the large uncertainty of the angular error estimates of these IceCube events, this source may be located at a different point in the sky. To avoid this problem, the full sky algorithm is restricted to a region of 20° around the proposed location. The likelihood used was the one presented in Ref. [5]. Because of the narrower size compared to the full sky search, the trial factor of this analysis is smaller. Apart from the point-source hypothesis, three Gaussian-like source extensions are considered (0.5°, 1° and 3°).

No significant cluster has been found. 90% C.L. upper limits for the four considered source extensions as a function of the declination of the source are represented in Figure 6. The possibility of a point source with a flux normalisation of 6×10^{-8} GeVcm^{-2}s^{-1} is discarded in the considered region with a CL higher than 90%. In this sense, the excess of events found by IceCube around the Galactic Centre would not be caused by a sole point-source with an E^{-2} source spectrum. In addition, a source width of 0.5° for declinations below −11° is also

Table 1. Pre-trial p-values, p, fitted number of source events, n_s, and 90% C.L. flux limits, Φ_ν^{90CL}, obtained for the 50 candidate sources. The fluxes are in units of 10^{-8} GeV cm^{-2}s^{-1}.

Name	α (°)	δ (°)	n_s	p	ϕ_ν^{90CL}	Name	α (°)	δ (°)	n_s	p	ϕ_ν^{90CL}
HESSJ0632+057	98.24	5.81	1.60	0.0012	4.40	HESSJ1912+101	-71.79	10.15	0.00	1.00	2.31
HESSJ1741-302	-94.75	-30.20	0.99	0.003	3.23	PKS0426-380	67.17	-37.93	0.00	1.00	1.59
3C279	-165.95	-5.79	1.11	0.01	3.45	W28	-89.57	-23.34	0.00	1.00	1.89
HESSJ1023-575	155.83	-57.76	1.98	0.03	2.01	MSH15-52	-131.47	-59.16	0.00	1.00	1.41
ESO139-G12	-95.59	-59.94	0.79	0.06	1.82	RGBJ0152+017	28.17	1.79	0.00	1.00	2.19
CirX-1	-129.83	-57.17	0.96	0.11	1.62	W51C	-69.25	14.19	0.00	1.00	2.32
PKS0548-322	87.67	-32.27	0.68	0.10	2.00	PKS1502+106	-133.90	10.52	0.00	1.00	2.31
GX339-4	-104.30	-48.79	0.50	0.14	1.50	HESSJ1632-478	-111.96	-47.82	0.00	1.00	1.33
VERJ0648+152	102.20	15.27	0.59	0.11	2.45	HESSJ1356-645	-151.00	-64.50	0.00	1.00	1.42
PKS0537-441	84.71	-44.08	0.24	0.16	1.37	1ES1101-232	165.91	-23.49	0.00	1.00	1.92
MGROJ1908+06	-73.01	6.27	0.21	0.14	2.32	HESSJ1507-622	-133.28	-62.34	0.00	1.00	1.41
Crab	83.63	22.01	0.00	1.00	2.46	RXJ0852.0-4622	133.00	-46.37	0.00	1.00	1.33
HESSJ1614-518	-116.42	-51.82	0.00	1.00	1.39	RCW86	-139.32	-62.48	0.00	1.00	1.41
HESSJ1837-069	-80.59	-6.95	0.00	1.00	2.09	RXJ1713.7-3946	-101.75	-39.75	0.00	1.00	1.59
PKS0235+164	39.66	16.61	0.00	1.00	2.39	SS433	-72.04	4.98	0.00	1.00	2.32
Geminga	98.31	17.01	0.00	1.00	2.39	1ES0347-121	57.35	-11.99	0.00	1.00	2.01
PKS0727-11	112.58	-11.70	0.00	1.00	2.01	VelaX	128.75	-45.60	0.00	1.00	1.33
PKS2005-489	-57.63	-48.82	0.00	1.00	1.39	HESSJ1303-631	-164.23	-63.20	0.00	1.00	1.43
PSRB1259-63	-164.30	-63.83	0.00	1.00	1.41	LS5039	-83.44	-14.83	0.00	1.00	1.96
HESSJ1503-582	-133.54	-58.74	0.00	1.00	1.41	PKS2155-304	-30.28	-30.22	0.00	1.00	1.79
PKS0454-234	74.27	-23.43	0.00	1.00	1.92	Galactic Centre	-93.58	-29.01	0.00	1.00	1.85
PKS1454-354	-135.64	-35.67	0.00	1.00	1.70	CentaurusA	-158.64	-43.02	0.00	1.00	1.36
HESSJ1834-087	-81.31	-8.76	0.00	1.00	2.06	W44	-75.96	1.38	0.00	1.00	2.23
HESSJ1616-508	-116.03	-50.97	0.00	1.00	1.39	IC443	94.21	22.51	0.00	1.00	2.50
H2356-309	-0.22	-30.63	0.00	1.00	2.35	3C454.3	-16.50	16.15	0.00	1.00	2.39

excluded. Since neutrinos with $E > 2\ PeV$ coming from an E^{-2} spectrum only contribute a 7% to the flux, these limits are barely affected by a cutoff on the order of the PeV.

8. Conclusions

The latest results of the ANTARES point-source search have been described using two complementary analyses. Firstly, a scan over the whole ANTARES visible sky. Secondly, a search over a list of 50 pre-selected neutrino candidate sources. The results found are compatible with a pure background hypothesis. In the first search, the post trial p-value of the most significant cluster is 2.7% (significance of 2.2σ). The largest excess found in the candidate source list study corresponds to HESS J0632+057 with a post-trial p-value of 6.1% (1.9σ). The computed flux upper limits are the most restrictive in a significant part of the Southern Sky. The possibility that the accumulation of 7 events reported by IceCube near the Galactic Centre is produced by a single point source has been excluded.

Acknowledgements

We gratefully acknowledge the financial support of the Spanish Ministerio de Economía y Competitividad (MINECO) grants FPA2012-37528-C02-01 and Consolider MultiDark CSD2009-00064, of the Generalitat Valenciana, PROMETEOII/2014/079, and of Universitat de València, Atracció de Talent.

References

[1] Aartsen M. G., Abbasi R., Abdou Y. et al. (IceCube Collaboration) 2013a, *Phys. Rev. Lett.*, **111**, 021103.
[2] Aartsen M. G., Abbasi R., Abdou Y. et al. (IceCube Collaboration) 2013c, *Science*, **342**, 6161, 1242856.

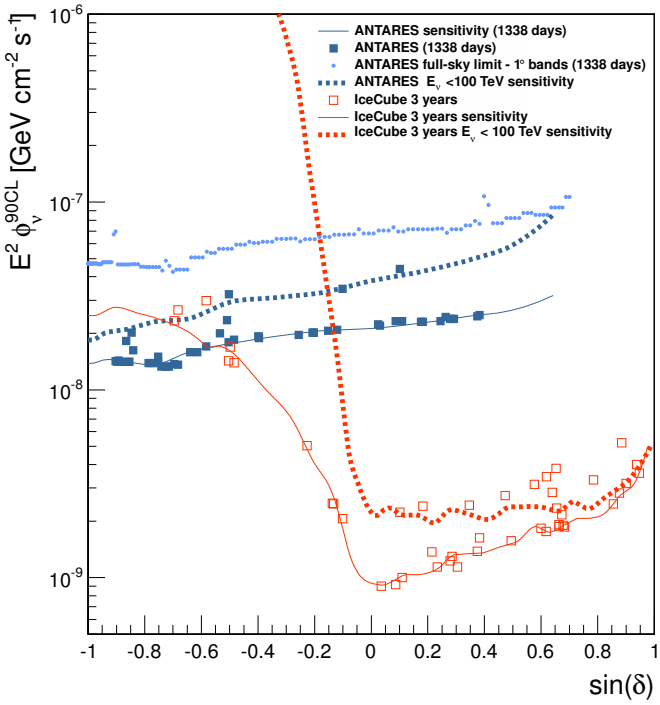

Figure 5. 90 % C.L. flux upper limits and sensitivities on the muon neutrino flux for six years of ANTARES data. IceCube results are also shown for comparison. The light-blue markers show the upper limit for any point source located in the ANTARES visible sky in declination bands of 1°. The solid blue (red) line indicates the ANTARES (IceCube) sensitivity for a point-source with an E^{-2} spectrum as a function of the declination. The blue (red) squares represent the upper limits for the ANTARES (IceCube) candidate sources. Finally, the dashed dark blue (red) line indicates the ANTARES (IceCube) sensitivity for a point-source and for neutrino energies lower than 100 TeV, which shows that the IceCube sensitivity for sources in the Southern hemisphere is mostly due to events of higher energy. The IceCube results were derived from [13].

[3] González-García M. C., Halzen F. & Niro V. 2014, *Astropart.Phys.*, **57-58**, 39.
[4] Ageron M., Aguilar J. A., Samarai I. Al et al. (ANTARES Collaboration) 2011, *Nucl. Instrum. Meth. A*, **656**, 11.
[5] Adrian-Martinez S., Samarai I.Al, Albert A. et al. (ANTARES Collaboration) 2012, *ApJ*, **760**, 53.
[6] Adrian-Martinez S., Samarai I.Al, Albert A. et al. (ANTARES Collaboration) 2013, *JCAP*, **1303**, 006.
[7] Brunner J. 2003, in VLVnT Workshop (Amsterdam), ANTARES simulation tools, ed. E. de Wolf (Amsterdam: NIKHEF), http://www.vlvnt.nl/proceedings.pdf
[8] Carminati G., Bazzotti M., Margiotta A. & Spurio M., *Comput. Phys. Commun.* (2008), **179**, 915.
[9] Bazzotti M., Carminati G., Margiotta A. & Spurio M., *Comput. Phys. Commun.* , **181**, 835.
[10] Agrawal V., Gaisser T. K., Lipari P. & Stanev T., *Phys. Rev. D*, **53**, 1314.
[11] Aguilar J. A., Albert A., Anton G. et al. (ANTARES Collaboration) 2010, *Astropart. Phys.*, **34**, 179.
[12] Barr G. D., Gaisser T. K., Robbins S. & Stanev T., *Phys. Rev. D*, **74**, 094009.
[13] Aartsen M. G., Abbasi R., Abdou Y. et al. (IceCube Collaboration) 2013b, *ApJ*, **779**, 132.
[14] Neyman J. 1937, *Phil. Trans. Royal Soc. London A*, **236**, 333.

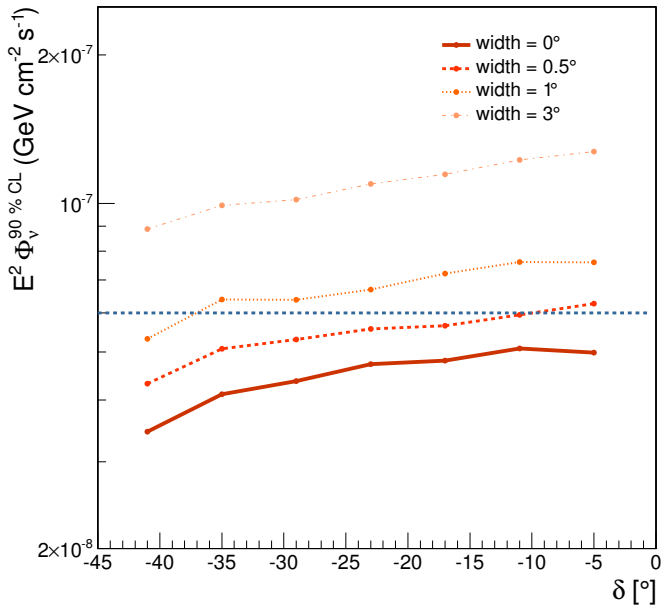

Figure 6. 90 % C.L. upper limits obtained for different source widths as a function of the declination. The blue horizontal dashed line corresponds to the signal flux given by [3].